ACS Chemical Neuroscience

RESEARCH ARTICLE

pubs.acs.org/acschemicalneuroscience

Molecular Microscopy of Brain Gangliosides: Illustrating their Distribution in Hippocampal Cell Layers

Benoit Colsch,[†] Shelley N. Jackson,[†] Sucharita Dutta,[‡] and Amina S. Woods*[,†]

[†]Structural Biology Unit, Cellular Neurobiology Section, NIDA IRP, NIH, Baltimore, Maryland 21224, United States

[‡]Thermo Fisher Scientific, San Jose, California, United States

Supporting Information

ABSTRACT: Gangliosides are amphiphilic molecules found in the outer layer of plasma membranes of all vertebrate cells. They play a major role in cell recognition and signaling and are involved in diseases affecting the central nervous system (CNS). We are reporting the differential distribution of ganglioside species in the rat brain's cerebrum, based on their ceramide associated core, and for the first time the presence of acetylation detected by matrix-assisted laser desorption/ionization (MALDI) mass spectrometry, which was used to map and image gangliosides with detailed structural information and histological accuracy. In the hippocampus, localization of the major species GM1, GD1, O-acetylGD1, GT1, and O-acetylGT1 depends on the sphingoïd base (d18:1 sphingosine or d20:1 eïcosasphingosine) in the molecular layer of the dentate gyrus (ML), which is made up of three distinct layers, the inner molecular layer (IML), which contains sphingosine exclusively, and the middle molecular layer (MML) and the outer molecular layer (OML) where eïcosasphingosine is the only sphingoïd base. These results demonstrate that there is a different distribution of gangliosides in neuronal axons and dendrites depending on the ceramide core of each layer. GM3, GM2, GD3, and GD2 contain sphingosine predominantly and are mainly present in body cell layers, which are made up of the pyramidal cell layer (Py) and the granular layer of the dentate gyrus (GL), in contrast with GQ1 and the O-acetylated forms of GD1, GT1, and GQ1 gangliosides, which contain both sphingoïd bases. However their distribution is based on the sialylated and acetylated oligosaccharide chains in the neuronal cell bodies.

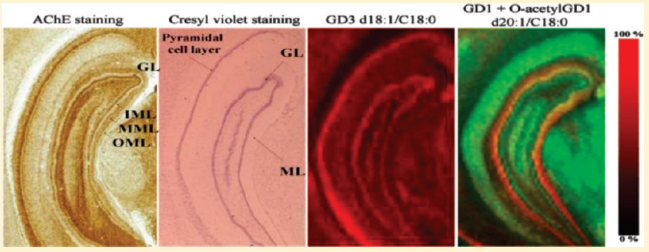

KEYWORDS: gangliosides, MALDI-imaging, molecular mapping, brain, hippocampus

Gangliosides are found in the outer plasma membrane layer of vertebrate cells. They are synthesized in the endoplasmic reticulum on a ceramide scaffold, which includes a fatty acid and a sphingoïd base.[1] Their glycosylation and sialylation take place in the Golgi apparatus.[2] They are one of the main constituents of lipid rafts[3,4] and play a major role in cell recognition and signaling.[5,6]

They are involved in diseases of the central nervous system such as GM1- and GM2-gangliosidosis affecting lysosomes [Sandhoff AB variant and Tay−Sachs],[7] and sialidosis where GM3 species are involved as in Alzheimer's disease where gangliosides bind Aβ peptides,[8] as well as in peripheral nervous system diseases such as Guillain−Barre syndrome.[9] Aberrant glycosylations are also found in cancerous cells.[10] Ganglioside antibodies, which recognize the sialylated oligosaccharide chain, are usually used to localize these molecules in brain tissue sections.[11,12] However no information on the ceramide core can be obtained by this approach thus highlighting the need for mass spectrometric imaging, which is a form of molecular imaging. It is a powerful and complementary method for mapping ganglioside species because it gives detailed information on the ceramide core using different matrices.[13−16] The present work demonstrates that we can also detect acetylation of gangliosides, which was not previously seen. Analysis of gangliosides by MALDI was always a challenge, because *in source* fragmentation of gangliosides results in the generation of GM1 from GD1 and GT1 through the loss of a sialic acid and is a major problem for the identification of these molecules.[17,18] Direct tissue analysis for imaging and mapping of GM1 in white matter gives misleading images of their distribution, which ends up looking like that of GD1. To minimize the loss of sialic acid moieties, high pressure in the MALDI source was suggested.[19] Direct profiling of ganglioside species in brain tissue sections by MALDI mass spectrometry to localize GM1 species in white matter was previously done.[20,21] In the current work, we minimized the impact of the loss of sialic acid moieties by using imaging software to normalize the signal, and thus our images reflect the correct GM1 localization and distribution in the cerebrum from MALDI MS data for the first time. Our images were correlated to immunostaining results from GM1 antibodies.[11,22] In this work, major and minor ganglioside species including acetylated forms were mapped in rat brain tissue sections and then with expanded details in the hippocampus area where our images show a high level of brain structural information.

Received: October 25, 2010
Accepted: January 20, 2011
Published: February 21, 2011

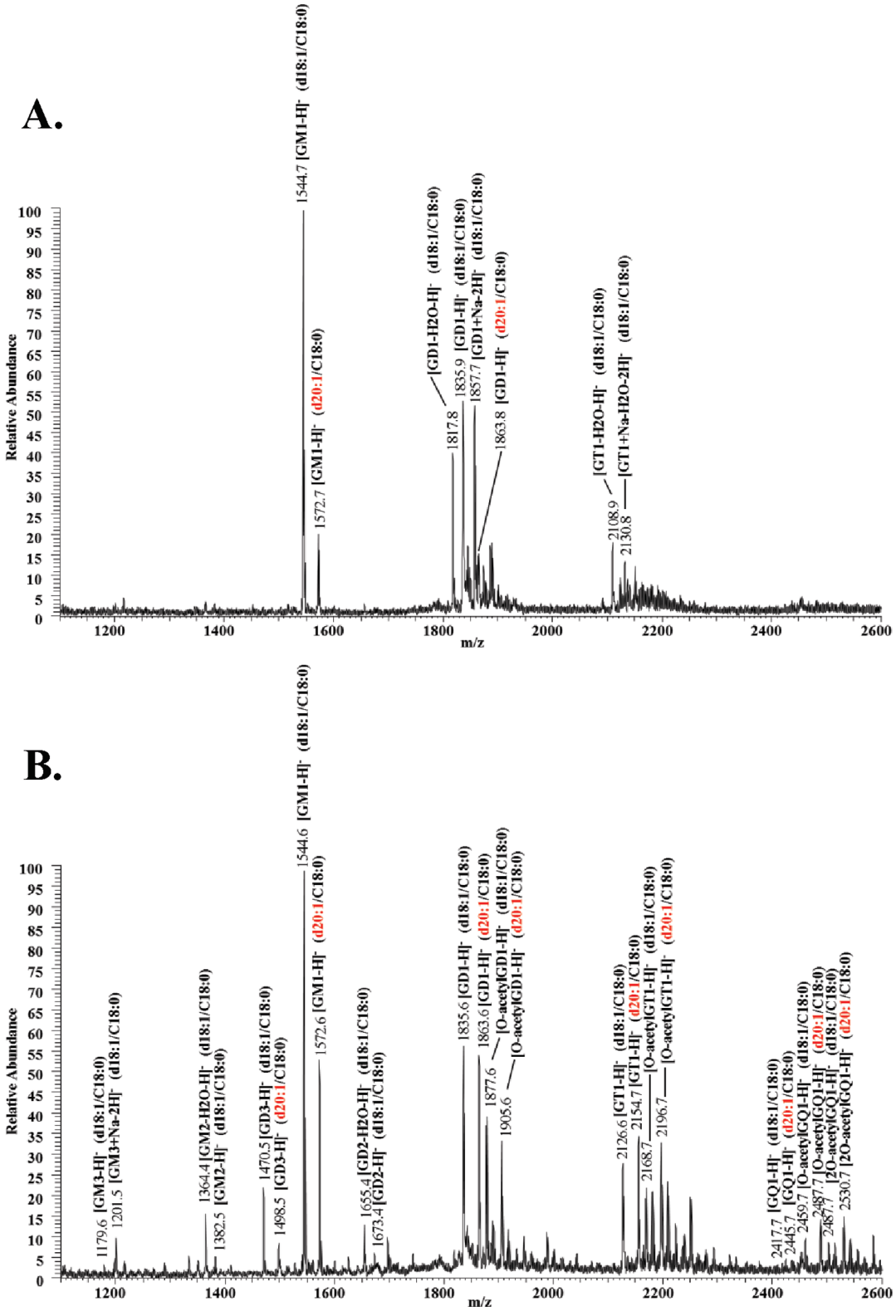

Figure 1. Mass spectrum of ganglioside species from rat cerebrum coronal tissue sections with (A) saturated DHA matrix and (B) saturated DHA/ammonium sulfate 125 mM/HFBA 0.05% using a MALDI-LTQ in negative ion mode. The presence of salt adducts such as GD1 + Na (m/z 1857.7) and loss of H_2O (m/z 1817.7 and m/z 2109.9) were observed for GD1 and GT1 gangliosides using saturated DHA (A). Only GM1, GD1, and GT1 gangliosides could be detected. GM1 (d18:1/C18:0; m/z 1544.7) represents the major ganglioside species due to *in source* fragmentation of GD1 and GT1 species resulting in the loss of sialic acid moieties. Addition of ammonium sulfate 3 mM in the matrix preparation increases the detection of minor and major ganglioside species. In addition, O-acetylated ganglioside species are also observed (B).

dx.doi.org/10.1021/cn100096h |*ACS Chem. Neurosci.* 2011, 2, 213–222

RESULTS AND DISCUSSION

Ganglioside Distribution in Rat Brain Tissue Sections by MALDI. MS spectra were acquired with a MALDI-LTQ mass spectrometer in negative ion mode using DHA and DHA/ammonium sulfate/HFBA matrix preparation. We previously reported the use of the DHA matrix for ganglioside analysis using a conventional axial MALDI-TOF.[15,20] Without ammonium sulfate, spectra of gangliosides are dominated by sodium adducts of GD1 and GT1 and their dehydrated forms. Minor and O-acetylated ganglioside species could not be detected (Figure 1A.). Similar results were obtained with the widely used lipid matrix DHB/0.1% TFA.[13] More recently, gold nanoparticles were used to detect and localize more gangliosides except GT1 and GQ1 species.[16] However addition of ammonium sulfate to the DHA matrix preparation minimized salt adducts and increased detection of deprotonated ions $[M - H]^-$ for all ganglioside species including minor and O-acetylated species. In addition, the loss of CO_2 reported with the use of the ATT matrix[23] was minimal or nonexistent. We did observe some loss of H_2O mainly from the minor species. Most major gangliosides such as GM1, GD1, GT1, and their O-acetylated forms (O-acetylGD1, O-acetylGT1), as well as the minor species GM3, GM2, GD2, GT2, GQ1, O-acetylGQ1, and 2O-acetylGQ1, were detected (Figure 1B). No O-acetylated GM1 species were seen under these conditions. This result suggests that the presence of acetylations on sialic acid moieties prevents *in source* fragmentation of O-acetylGD1, O-acetylGT1.

Structural Elucidation of Gangliosdies by ESI-MS^n Analysis. In order to confirm the assignments in Figure 1, MS^n analysis was conducted using an ESI-LTQ Orbitrap in negative ion mode with both CID and HCD fragmentation. A total ganglioside extract from brain tissue sections, obtained from the same bregma as the imaged tissue in this study, was analyzed. Figure 2 illustrates product-ion spectra for the doubly charged molecular ion for GD1 (d18:1/C18:0) at m/z 917.48 (Figure 2A) and O-acteylGD1 (d18:1/C18:0) at m/z 938.50 (Figure 2B) in negative ion mode with HCD fragmentation. In both spectra, we observed a sequential fragmentation of the headgroup (oligosaccharide chain and sialic acid moieties) in agreement with Domon and Costello[24] and represented by peaks at m/z 1544.87, 1253.77, 1091.72, 888.64, 726.59, 564.54, and 283.26. The representative sialic acid peak at m/z 290.1 and that representing two sialic acid moieties m/z 581.2 were observed in both spectra. The presence of one acetyl group (+42 Da) in the O-acetylGD1 (d18:1/C18:0) ganglioside species and its attachment to the sialic acid moiety was confirmed by the presence of mass peaks 1586.88, 1295.81, 623.19, and 332.10.[25] Additional confirmation of O-acetylation was obtained by MS^3 of 581.2 $[2SA - H]^-$ (Figure 2C) and 623.2 $[2O\text{-acetylSA} - H]^-$ (Figure 2D). As expected, the MS^3 spectrum of 581.2 contained only one major fragment peak at 290.1 $[SA - H]^-$, while the MS^3 spectrum of 623.2 contained several fragment peaks with the two major peaks at 332.2 $[O\text{-acetylSA} - H]^-$ and 290.2 $[SA - H]^-$. This result further substantiated the assignment of one acetyl group attached to a sialic acid residue for the peak at m/z 938.50. All peak assignments for acetylation were confirmed by MS^n fragmentation, and the results are listed in Table 1.

Imaging Mass Spectrometry of Major and Minor Ganglioside Species in Rat Brain Tissue Sections. We imaged ganglioside distribution in a rat brain section corresponding to plate 81 (interneural 3.24 mm, bregma −5.76 mm) of the coronal

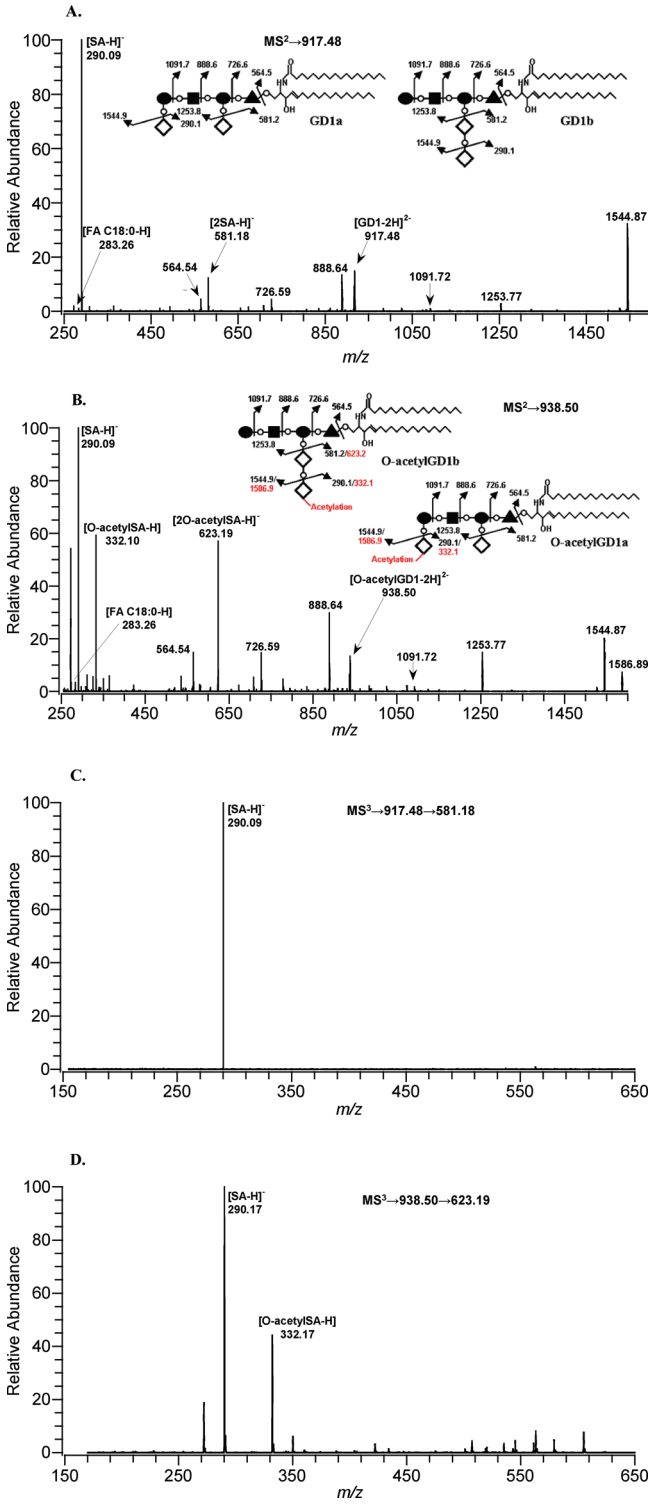

Figure 2. Product-ion spectra of the doubly charged ion $[M - 2H]^{2-}$ GD1 (d18:1/C18:0) ganglioside (m/z 917.48) (A) and the doubly charged ion $[M - 2H]^{2-}$ O-acetylGD1 (d18:1/C18:0) ganglioside (m/z 938.50) (B) and MS^3 spectra of (C) m/z 581.18 $[2SA - H]^-$ and (D) m/z 623.19 $[2O\text{-acetylSA} - H]-$: (▲) glucose (Glc); (●) galactose (Gal); (■) *N*-acetylgalactosamine (GalNac); (◇) sialic acid (SA/NeuAc).

location from *The Rat Brain in Stereotaxic Coordinates*.[26] A plate of an acetylcholinesterase staining from Paxinos and Watson's Atlas show the three distinct layers (IML, MML, OML) forming

Table 1. Assignment of Ganglioside Species by MS^n

class	mass peak (m/z)[a]	fragment ions[b]	fatty acid	sphingoid base	*O*-acetyl
GM_1	$[M - H]^-$ = 1544.87	$[1253.78]^-$, $[1091.72]^-$, $[888.64]^-$, $[726.59]^-$, $[564.54]^-$	C18:0	d18:1	0
GM_1	$[M - H]^-$ = 1572.90	$[1281.81]^-$, $[916.67]^-$, $[754.62]^-$, $[592.57]^-$	C18:0	d20:1	0
GD_1	$[M - 2H]^{2-}$ = 917.48	$[1544.87]^-$, $[1253.77]^-$, $[1091.72]$, $[888.64]^-$, $[726.59]^-$, $[581.18]^-$, $[564.54]^-$, $[290.09]^-$	C18:0	d18:1	0
GD_1	$[M - 2H]^{2-}$ = 931.49	$[1572.90]^-$, $[1281.81]^-$, $[1119.75]^-$, $[916.67]^-$, $[754.62]^-$, $[592.57]^-$, $[581.18]^-$, $[290.09]^-$	C18:0	d20:1	0
GD_1	$[M - 2H]^{2-}$ = 938.50	$[\mathbf{1586.88}]^-$, $[1544.87]^-$, $[\mathbf{1295.81}]^-$, $[1253.77]^-$, $[1091.72]^-$, $[888.64]^-$, $[726.59]^-$, $[\mathbf{623.19}]^-$, $[581.19]^-$, $[564.54]^-$, $[\mathbf{332.10}]^-$, $[290.09]^-$	C18:0	d18:1	1
GD_1	$[M - 2H]^{2-}$ = 952.52	$[\mathbf{1614.92}]^-$, $[1572.90]^-$, $[\mathbf{1323.84}]^-$, $[1281.81]^-$, $[1119.75]^-$, $[916.67]^-$, $[754.62]^-$, $[\mathbf{623.19}]^-$, $[592.57]^-$, $[581.18]^-$, $[\mathbf{332.10}]^-$, $[290.09]^-$	C18:0	d20:1	1
GT_{1b}	$[M - 2H]^{2-}$ = 1063.03	$[1836.97]^-$, $[1544.87]^-$, $[1253.77]^-$, $[917.48]^{2-}$, $[888.64]^-$, $[581.18]^-$, $[564.54]^-$, $[290.09]^-$	C18:0	d18:1	0
GT_{1b}	$[M - 2H]^{2-}$ = 1077.04	$[1865.00]^-$, $[1572.90]^-$, $[1281.80]^-$, $[931.49]^{2-}$, $[916.67]^-$, $[754.62]^-$, $[592.57]^-$, $[581.18]^-$	C18:0	d20:1	0
GT_{1b}	$[M - 2H]^{2-}$ = 1084.05	$[\mathbf{1877.98}]^-$, $[1835.96]^-$, $[\mathbf{1586.89}]^-$, $[1544.87]^-$, $[1253.77]^-$, $[1062.04]^{2-}$, $[\mathbf{938.48}]^{2-}$, $[917.48]^{2-}$, $[888.64]^-$, $[726.59]^-$, $[\mathbf{623.19}]^-$, $[564.54]^-$, $[\mathbf{332.10}]^-$	C18:0	d18:1	1
GT_{1b}	$[M - 2H]^{2-}$ = 1098.06	$[\mathbf{1906.01}]^-$, $[1863.99]^-$, $[\mathbf{1614.92}]^-$, $[1572.90]^-$, $[1281.80]^-$, $[1076.05]^{2-}$, $[\mathbf{952.50}]^{2-}$, $[931.49]^{2-}$, $[916.67]^-$, $[754.62]^-$, $[\mathbf{623.19}]^-$, $[\mathbf{332.10}]^-$	C18:0	d20:1	1
GQ_{1b}	$[M - 2H]^{2-}$ = 1208.57	$[1835.96]^-$, $[1544.87]^-$, $[1063.03]^{2-}$, $[917.48]^{2-}$, $[888.63]^-$, $[581.19]^-$, $[564.54]^-$	C18:0	d18:1	0
GQ_{1b}	$[M - 2H]^{2-}$ = 1222.59	$[1864.00]^-$, $[1572.91]^-$, $[1281.81]^-$, $[1077.04]^{2-}$, $[931.50]^{2-}$, $[916.67]^-$, $[754.61]^-$, $[581.19]^-$	C18:0	d20:1	0
GQ_{1b}	$[M - 2H]^{2-}$ = 1230.08	$[\mathbf{1877.98}]^-$, $[1835.96]^-$, $[1544.87]^-$, $[1253.77]^-$, $[1063.03]^{2-}$, $[917.48]^{2-}$, $[\mathbf{623.20}]^-$, $[581.18]^-$	C18:0	d18:1	1
GQ_{1b}	$[M - 2H]^{2-}$ = 1244.10	$[\mathbf{1906.01}]^-$, $[1864.00]^-$, $[1572.91]^-$, $[1281.81]^-$, $[\mathbf{1098.05}]^{2-}$, $[1077.04]^{2-}$, $[931.50]^{2-}$, $[916.68]^-$, $[754.62]^-$, $[\mathbf{623.20}]^-$, $[581.19]^-$	C18:0	d20:1	1
GQ_{1b}	$[M - 2H]^{2-}$ = 1251.59	$[\mathbf{1920.07}]^-$, $[\mathbf{1877.98}]^-$, $[1836.98]^-$, $[\mathbf{1586.90}]^-$, $[1544.87]^-$, $[1253.78]^-$, $[\mathbf{1084.54}]^{2-}$, $[1062.04]^{2-}$, $[\mathbf{938.49}]^{2-}$, $[917.48]^{2-}$, $[888.64]^-$, $[726.59]^-$, $[\mathbf{665.21}]^-$, $[\mathbf{623.20}]^-$	C18:0	d18:1	2
GQ_{1b}	$[M - 2H]^{2-}$ = 1265.61	$[\mathbf{1948.06}]^-$, $[\mathbf{1906.01}]^-$, $[1864.00]^-$, $[1572.91]^-$, $[1281.81]^-[1119.76]^-$, $[\mathbf{1098.05}]^{2-}$, $[1076.05]^{2-}$, $[916.68]^-$, $[754.62]^-$, $[\mathbf{665.20}]^-$, $[\mathbf{623.20}]^-$	C18:0	d20:1	2

[a] Mass peaks are monoistopic mass. [b] Bold text represents fragment peaks that contain *O*-acetyl group.

dx.doi.org/10.1021/cn100096h |*ACS Chem. Neurosci.* 2011, 2, 213–222

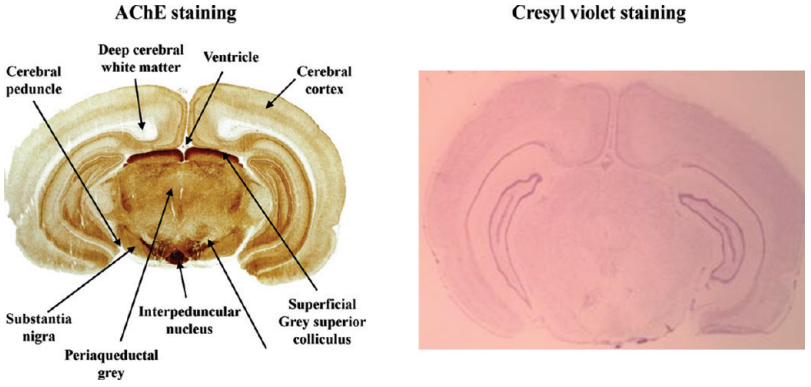

Figure 3. AChE staining and cresyl violet staining of a rat brain section corresponding to plate 81 (interneural 3.24 mm, bregma −5.76 mm) of the coronal location from *The Rat Brain in Stereotaxic Coordinates*.[26] This area was used for all the images in this study.

the molecular layer (ML) of the hippocampus' dentate gyrus, and a cresyl violet staining was also performed to localize the body cell layers such as the pyramidal cell layers (Py) and the granular layer of the dentate gyrus (GL) of the hippocampus (Figure 3). Except for the GM1 localization, all other ganglioside species were mapped using a normalization procedure (mass range species/total ion current (TIC)) to increase the visual acquity of the images (Figure 4A). The *in source* fragmentation of GD1 and GT1 results in the loss of sialic acids moieties, thus giving misleading images (maps) of the distribution and localization of GM1. After application of software for signal normalization (GM1 mass range/GD1 mass range), GM1 (d18:1/C18:0; m/z 1544.7) is clearly detected in the corpus callosum, and its distribution corresponds to that of immunostaining results obtained with GM1 antibody[11,22] (Figure 4B). The normalization procedure will be explained in the Methods section. The major brain gangliosides (GM1, GD1, and GT1) and GQ1s were mapped (Figure 5A.). A differential distribution was observed in brain coronal sections depending on the sphingoïd base of each species. They are also seen in the substantia nigra, cerebral peduncle, hippocampus, and midbrain. However, the GM1 (d20:1/C18:0) species (m/z 1572.7) is minimally present in the corpus callosum and midbrain and is mostly found in the hippocampus and the substantia nigra, a result that could not have been deduced from immunostaining because it does not distinguish between GM1 (d18:1/C18:0) and GM1 (d20:1/C18:0) isoforms. In addition, mass spectrometry could not previously distinguish between GM1 generated from *in source* fragmentation of GD1 and GT1. The GD1 ganglioside (d18:1/C18:0) species (m/z 1835.7) is not expressed in the corpus callosum and part of the midbrain region but is present in the hippocampus, cortex, periaqueductal gray area, interpeduncular nucleus, and substantia nigra, while the GD1 (d20:1/C18:0) ganglioside species (m/z 1863.7) is mainly located in the cortex, superficial gray superior colliculus, and part of the hippocampus. The distributions of GT1 species are similar to GD1 species in function of their sphingoïd base. The elusive GQ1 (d18:1/C18:0) ganglioside species (m/z 2417.8) was mapped in the periaqueductal gray area, dorsal subiculum, superficial gray superior colliculus, and minimally in GL of the hippocampus, while the GQ1 (d20:1/C18:0) species (m/z 2445.8) is mostly present in the corpus callosum.

One of each of the minor ganglioside species with the same ceramide core (d18:1/C18:0) is also shown (Figure 5B): GD2 (m/z 1673.7), GT3 (m/z 1761.7), and GT2 (m/z 1964.7), which

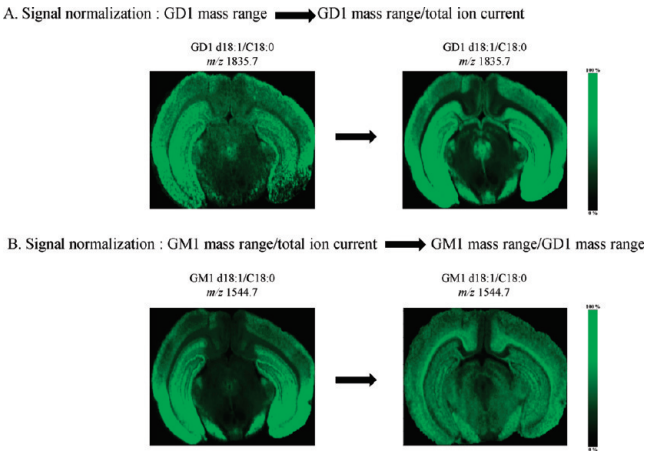

Figure 4. In order to improve the visual quality of the images, the m/z range of interest was normalized by dividing by total ion current (TIC) for the mass spectra for all ganglioside species except the GM1 (A). Due to *in source* fragmentation of complex ganglioside species (mostly GD1 due to the loss of one sialic acid moiety), the mapping of GM1 is flawed and represents principally the GD1 distribution. Another signal normalization was performed using the imaging software resulting in the true distribution of GM1 species corresponding to the immunostaining data (B).[22]

are mostly present in the corpus callosum, midbrain, and hippocampus but not in the substantia nigra, periaqueductal gray, and interpeduncular nucleus. In contrast GM3 (m/z 1179.7) and GM2 (m/z 1382.7) ganglioside species are expressed in the ventricles and hippocampus areas. The GM2 signal at the edge of the tissue section is not due to GM2 distribution. It is background noise from the stainless steel plate. In addition, GM3 is also found in the corpus callosum. The GD3 (m/z 1470.7) ganglioside species is mainly present in the superficial gray superior colliculus, periaqueductal gray area, and interpeduncular nucleus. In the hippocampus area, all minor ganglioside species are localized in Py and GL except for the GT3 species.

Localization of O-Acetylated Ganglioside Species. In addition to differentiating gangliosides based on their ceramide core structure. Another differential distribution due to one or two acetylations of sialic acids moieties was also delineated (Figure 6).

The acetylated ganglioside species, of which this is the first mapping by imaging mass spectrometry, are mainly located in the hippocampus area and the cerebral cortex for the d18:1 sphingosine base such as O-acetylGD1 (m/z 1877.7) and O-acetylGT1

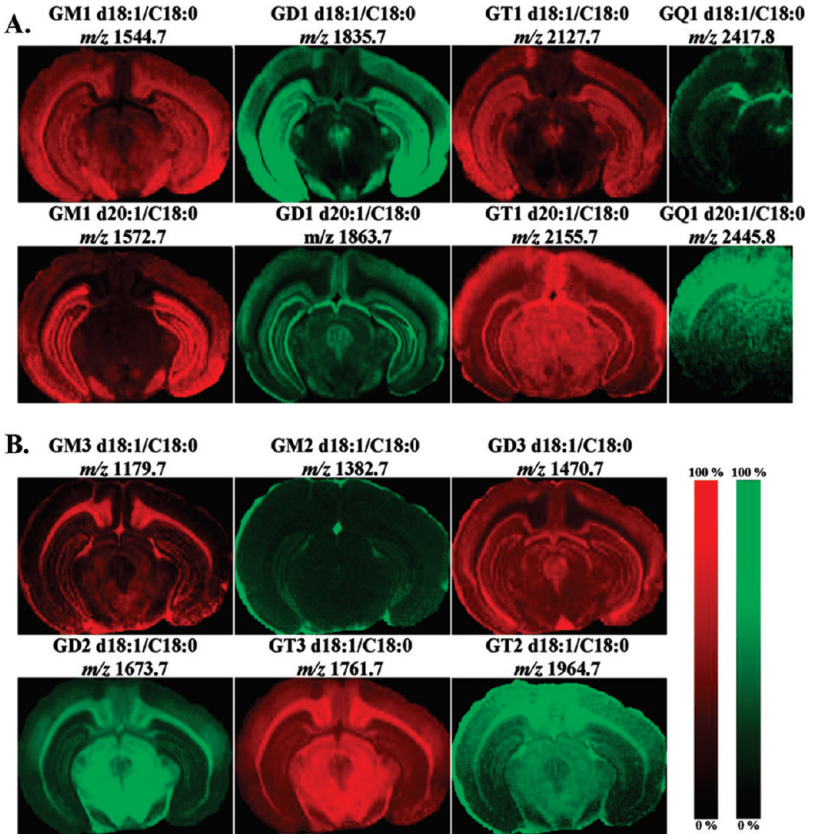

Figure 5. MALDI imaging mass spectrometry of minor and major ganglioside species using saturated DHA/ammonium sulfate 125 mM/HFBA 0.05% using a MALDI-LTQ in negative ion mode. Major ganglioside species (GM1, GD1, and GT1) and GQ1 species were mapped based on their ceramide core made of sphingosine (d18:1) or eïcosasphingosine (d20:1). GM1 ganglioside species are mapped after signal normalization using the imaging software (A). A differential distribution of minor ganglioside species is also observed using this matrix preparation and shows different localization in function of the degree of glycosylation and sialylation for these species (B).

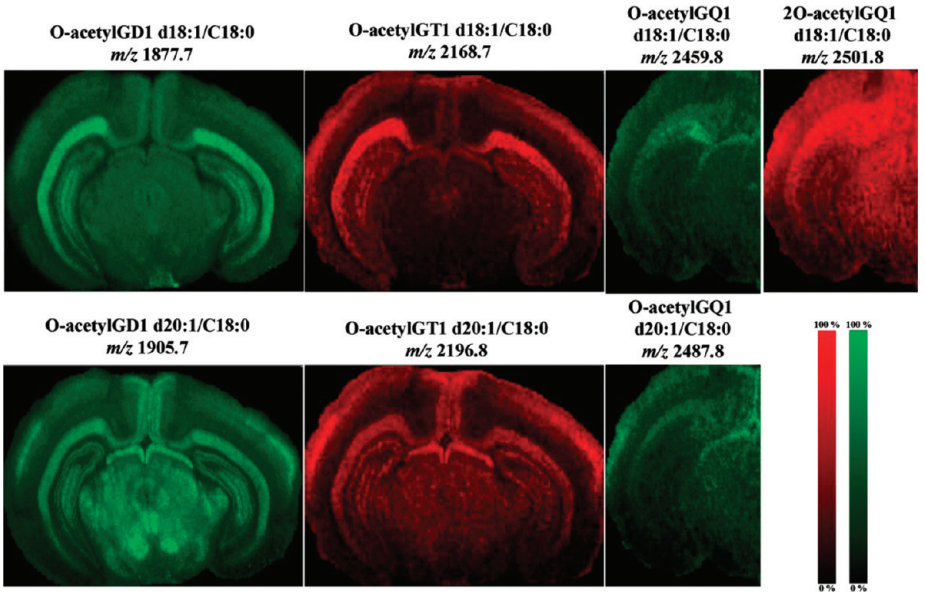

Figure 6. MALDI imaging mass spectrometry of O-acetylated gangliosides using saturated DHA/ammonium sulfate 125 mM/HFBA 0.05% using a MALDI-LTQ in negative ion mode. The presence of one or two acetyl groups on sialic acid moieties induced a different distribution than that of the nonacetylated ganglioside species.

(*m*/*z* 2168.7). O-acetylGD1 (*m*/*z* 1905.7) and O-acetylGT1 (*m*/*z* 2196.7) ganglioside species that include the eïcosasphingosine d20:1 are also located in the hippocampus area, cortex, and midbrain, mainly in the red nucleus and superficial gray superior

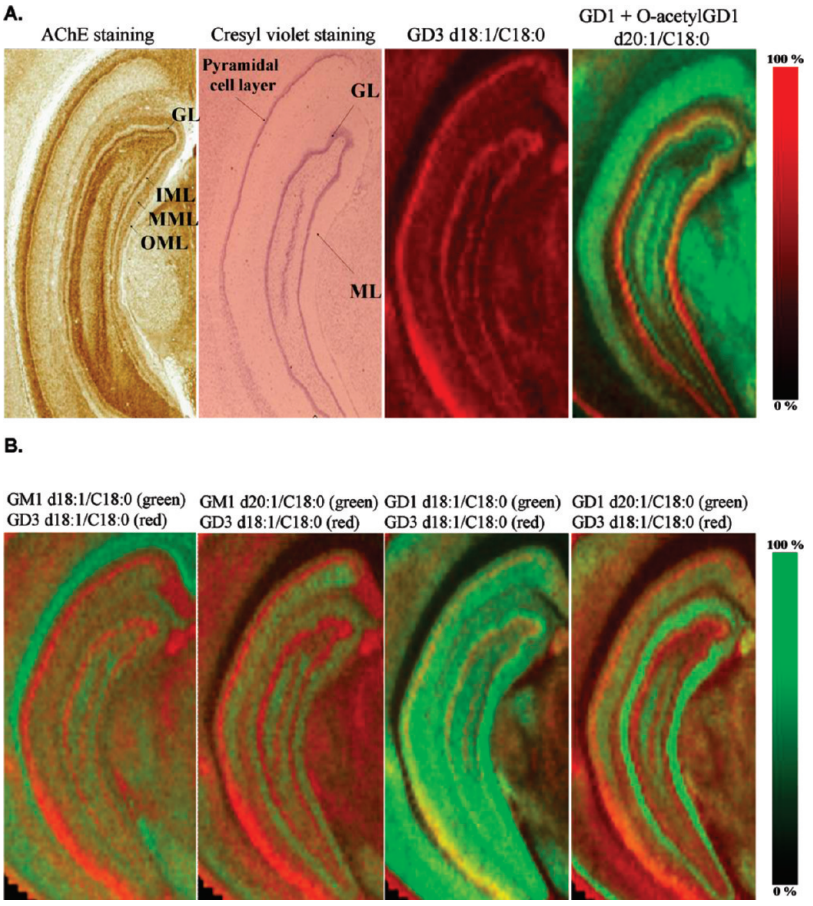

Figure 7. MALDI imaging of ganglioside species in the hippocampus area. GD3 (d18:1/C18:0) ganglioside (m/z 1470.7) is chosen as reference to localize Py and GL layers in the hippocampus and compared with the cresyl violet staining. The three layers in ML can be observed with a combination image of GD1 (d20:1/C18:0) ganglioside species (m/z 1863.7) shown in red and O-acetylGD1 (d20:1/C18:0) ganglioside species (m/z 1905.7) in green. The green layer represents the GL and contains only the O-acetylGD1. The black layer represents the IML and does not contain either ganglioside species. The yellow layer (MML) contains both, while the red layer (OML) contains only the GD1 ganglioside specie (A). The major ganglioside species (GM1, GD1) were merged with the GD3 in one image to determine their precise location (B).

colliculus. Unlike GD1 and GT1 ganglioside species, the presence of an acetyl group does not change the distribution for the GQ1 ganglioside species. GQ1 and O-acetylGQ1 species have the same distribution in rat brain depending on the sphingoïd base. However, the 2O-acetylGQ1 (d18:1/C18:0) ganglioside (m/z 2501.8) does not appear in the superficial gray superior colliculus, but mostly in the corpus callosum and to a lesser extent in the GL of the hippocampus.

Imaging Mass Spectrometry of Gangliosides in Hippocampal Cell Layers. We focused next on the hippocampus area to localize ganglioside species with a high level of structural accuracy (Figure 7). GD3 ganglioside (d18:1/C18:0) (m/z 1470.7) was chosen as reference to localize the GL in the hippocampus. A cresyl violet staining was performed to confirm its presence in the GL. The three distinct layers IML, MML, and OML present in the ML of the hippocampus can be visualized with AChE staining as seen in *The Rat Brain in Stereotaxic Coordinates*.[26] According to the width measurements carried out directly on the rat brain section optical image, the GL of the hippocampus represents a width of 60−150 μm, while the Py represents a width of 30−50 μm and the ML of the hippocampus a width between 250 and 350 μm, containing three internal layers (Figure 7A.). A combination image of the major GD1 (d20:1/C18:0) ganglioside (m/z 1863.7) depicted in red and the minor O-acetylGD1 (d20:1/C18:0) ganglioside (m/z 1905.7) in green shows the four different layers present in the hippocampal area. The GL is featured in green and contains only the O-acetylGD1 ganglioside. The IML is featured in black and does not contain either ganglioside species, while the MML layer featured in yellow contains both gangliosides, and the OML in red contains only GD1. The minor GD3 ganglioside localization (red color) was merged with the major GM1 and GD1, which contain both sphingosine and eïcosasphingosine (green color), to determine their differential distribution in the hippocampus area (Figure 7B.). According to these results, neither GM1 species is located in the body cell layers (Py and GL), but the GM1 (d18:1/C18:0) ganglioside (m/z 1544.7) is present to some extent in the IML, lacunosum moleculare, oriens and radiatum layers, and field CA1, in contrast to the GM1 (d20:1/C18:0) ganglioside (m/z 1572.7), some of which is located in the MML and OML but not in the IML and lacunosum moleculare. The field CA1, oriens, and radiatum layers are also positive for this GM1 species. Disialoganglioside d18:1/C18:0 (m/z 1835.7) and d20:1/C18:0 (m/z 1863.7) species have approximately the same localization as monosialoganglioside species as a function of their sphingoïd base. However, in contrast to the GM1 (d20:1/C18:0) ganglioside, GD1 (d20:1/C18:0) is mainly present in the MML and OML layers.

dx.doi.org/10.1021/cn100096h |*ACS Chem. Neurosci.* 2011, 2, 213–222

According to these results, the qualitative localization of ganglioside species depend on (i) the degree of glycosylation and sialylations, (ii) the ceramide structure defined by the presence of either major sphingoïd base d18:1 or d20:1, (iii) the presence of acetylated sialic acid moieties, which do not seem to fragment *in source*. Immunostaining using antibodies, lectins, or toxins to detect ganglioside molecules recognizes the headgroup of these molecules, which includes the sialylated oligosaccharide chain and depends on the degree of glycosylation and sialylation. This technique has a high level of sensitivity and is widely used in biology. However, imaging mass spectrometry is a complementary method that recognizes all components of a molecule, headgroup as well as ceramide core. Adding the information obtained by molecular fragmentation makes it an unparalleled and incontrovertible source of structural delineation; thus we designated the technique with the title of "molecular microscopy". Furthermore, several antiganglioside antibodies recognize both nonacetylated and acetylated forms of a ganglioside, while other antibodies recognize either nonacetylated or acetylated forms thus generating much confusion. O-Acetylation of ganglioside sialic acid moieties make them susceptible to alkaline hydrolysis. Studies using alkaline conditions suggested the presence of O-acetylation on a specific terminal α2−8-linked sialic acid residue in murine brain.[27−29] These modifications strongly influence the physiological properties of sialic acid moieties.[30,31] *In source* fragmentation of sialic acids, which is often alluded to in the literature,[19,32] was also observed. However the use of imaging software made correction of the flawed GM1 localization possible, so that the image corresponds to the native GM1 rather than the GM1 generated by the loss of sialic acid from GD1 and GT1 species often encountered in MALDI imaging. The next challenge in ganglioside imaging is the differentiation and mapping of isomers such as GD1a and GD1b. Furthermore, this matrix preparation that detects minor and major ganglioside species might also be useful for glycosphingolipid analysis in biological fluids, from animal models of neurological diseases and tumors where O-acetylated gangliosides are involved.[33]

METHODS

Chemicals. Heptafluorobutyric acid (HFBA) and 2,6-dihydroxyacetophenone (DHA) were purchased from Fluka (St. Louis, MO). Ethanol was purchased from the Winner-Graham Company (Cockeysville, MD). Distilled water was obtained from a Picopure2 system (Hydro, Rockville, MD). Ammonium sulfate was obtained from J.T Baker (Phillipsburg, NJ).

Tissue Preparation. All the animal work in this study abides by the Guide for the Care and Use of Laboratory Animals (NIH). Adult Sprague−Dawley rat brains were removed from the skull and frozen in dry ice chilled isopentane. The brain was attached to the cryostat specimen disk using ice slush made from distilled water. Frozen brain tissue was cut into thin sections (18 μm thickness) using a cryostat (Leica Microsystems CM3050S, Bannockburn, IL) at −25 °C (cryochamber temperature) and −16 °C (specimen cooling temperature). For imaging, coronal tissue slices were directly deposited on the MALDI target plate and brought to room temperature before matrix coating. Total lipids were extracted from two rat brain coronal sections (∼2 mg) using modified Folch extraction method.[34] We confirmed our peak assignments by MS^n using an ESI-LTQ. The upper phase (aqueous phase) containing enriched ganglioside species was desalted with C18-bonded silica gel columns (Supelco, Bellefonte, PA, USA) according to Williams and McCluer,[35] dried under a gentle stream of nitrogen, and redissolved in methanol and then kept at −20 °C until mass spectrometric analysis.

Mass Spectrometers. *MALDI-LTQ.* A LTQ XL (Thermo Fisher Scientific, San Jose, CA) with a MALDI source was used to acquire the MALDI imaging data. Samples are ionized with a nitrogen laser (λ = 337 nm, rep. rate = 60 Hz). All data was acquired in negative ion mode. For GM3, GM2, GD3, GM1, GT3, GD1, and O-acetylGD1 species, data was recorded in the m/z range of 1100−2000, and the imaging parameters were 2 microscans/step with 10 laser shots per step at a laser energy of 20 μJ and a raster step size of 80 μm. GT1 and O-acetylGT1 species were analyzed in the m/z range of 2110−2220 with the following imaging parameters: 2 microscans/step, 10 laser shots per step, laser energy of 25 μJ, and a raster step size of 80 μm. For GQ1, O-acetylGQ1, and 2O-acetylGQ1 species, a m/z range of 2410−2510 was used with the following imaging settings: 2 microscans/step, 30 laser shots per step, laser energy of 25 μJ, and a raster step size of 80 μm. The two-dimensional ion density maps (MALDI images) were generated using the ImageQuest software (Thermo Scientific). In this software, a m/z range is plotted for signal intensity for each pixel (mass spectrum) across a given area (tissue section).

ESI-LTQ Orbitrap Velos. A LTQ Orbitrap Velos (Thermo Fisher Scientific, San Jose, CA) with an ESI source was used to analyze the brain ganglioside extract. Data was recorded in negative ion mode with a sample flow rate of 5 μL/min. MS^n analyses in collision-induced dissociation (CID) and high-energy collisional dissociation (HCD) mode were conducted on each ganglioside species in order to confirm the structure.

Matrix Preparation and Matrix Application System. Due to its rapid sublimation under high vacuum,[36,37] 2,6-dihydroxyacetphenone (DHA) matrix could not be used for imaging mass spectrometry. However, we changed the chemical properties of the matrix preparation by adding HFBA, which increased its stability in vacuum thus allowing its use for tissue imaging. We previously mapped some gangliosides using a chemical inkjet printer to deposit the matrix preparation,[15] which is the matrix deposition method of choice when imaging small molecules and for profiling. However the size of the matrix spots can limit the resolution. So in this study, we used an artistic airbrush to coat the tissue sections with matrix, because gangliosides are embedded in the plasma membrane and could not be delocalized like small molecules are when using the airbrush spraying technique. DHA was prepared as a saturated solution in 50% ethanol with 125 mM ammonium sulfate and 0.05% heptafluorobutyric acid (HFBA). Recently, it was shown that by addition of ammonium sulfate and HFBA to DHA matrix solutions, its stability in vacuum can be extended thus allowing imaging experiments to be conducted. The matrix solution was sprayed on the tissue sections with an artistic airbrush to produce a uniform coating of the matrix. To improve the matrix coating and limit evaporation, the spraying was done in a cold room (+4 °C).

Signal Normalization Procedure Using ImageQuest Software (Thermo Scientific). In order to improve the visual quality of the images, the m/z range of interest was normalized by dividing by total ion current (TIC). This was previously done in imaging to improve image quality.[38] Due to the in source fragmentation of GD1 yielding GM1, the GM1 m/z range was divided by the GD1 m/z range in order to normalize the effects of this fragmentation. This processing was only done for GM1 species.

ASSOCIATED CONTENT

Supporting Information. Additional MS^n data used to produce Table 1. This material is available free of charge via the Internet at http://pubs.acs.org.

AUTHOR INFORMATION

Corresponding Author

*Tel: 443-740-2747. Fax: 443-740-2144. E-mail: awoods@mail.nih.gov.

Author Contributions

B.C., S.N.J., and A.S.W. designed the research. B.C., S.N.J., and S. D. performed the research and analyzed the data. B.C., S.N.J., and A.S.W wrote the paper.

Funding Sources

This research was supported by the Intramural Research Program of the National Institute on Drug Abuse, NIH. We thank the Office of National Drug Control Policy (ONDCP) for instrumentation funding, without which this and other projects could not have been accomplished.

■ ACKNOWLEDGMENT

We thank Elsevier publishing for allowing us to use a plate from their Atlas *The Rat Brain in Stereotaxic Coordinates*.

■ ABBREVIATIONS

DHA, 2,6-dihydroxyacetophenone; DHB, 2,5-dihydroxybenzoic acid; ESI, electrospray ionization; GL, granular layer of dentate gyrus; HFBA, heptafluorobutyric acid; IML, inner molecular layer of dentate gyrus; LTQ, linear trap quadrupole; ML, molecular layer of dentate gyrus; MML, middle molecular layer of dentate gyrus; MALDI, matrix-assisted laser desorption/ionization; OML, outer molecular layer of dentate gyrus; TFA, trifluoroacetic acid; Py, pyramidal cell layer; TIC, total ion current

■ REFERENCES

(1) Merill, A. H. (2002) De novo sphingolipid biosynthesis: A necessary, but dangerous, pathway. *J. Biol. Chem. 277*, 25843–25846.

(2) Kolter, T., Proia, R. L., and Sandhoff, K. (2002) Combinatorial ganglioside biosynthesis. *J. Biol. Chem. 277*, 25859–25862.

(3) Simons, K., and Toomre, D. (2000) Lipid rafts and signal transduction. *Nat. Rev. Mol. Cell Biol. 1*, 31–39.

(4) Sonnino, S., Mauri, L., Chigorno, V., and Prinetti, A. (2007) Gangliosides as components of lipid membrane domains. *Glycobiology 17*, 1R–13R.

(5) Hakomori, S., and Igarashi, Y. (1995) Functional role of glycosphingolipids in cell recognition and signaling. *J. Biochem. 118*, 1091–1103.

(6) Lopez, P. H. H., and Schnaar, R. L. (2009) Gangliosides in cell recognition and membrane protein regulation. *Curr. Opin. Struct. Biol. 19*, 549–557.

(7) Kolter, T., and Sandhoff, K. (2005) Principles of lysosomal membrane digestion: Stimulation of sphingolipid degradation by sphingolipid activator proteins and anionic lysosomal lipids. *Annu. Rev. Cell Dev. Biol. 21*, 81–103.

(8) Ariga, T., McDonald, M. P., and Yu, R. K. (2008) Role of ganglioside metabolism in the pathogenesis of Alzheimer's disease-a review. *J. Lipid Res. 49*, 1157–1175.

(9) Willison, H. J. (2007) Gangliosides as targets for autoimmune injury to the nervous system. *J. Neurochem. 103*, 143–149.

(10) Hakomori, S. (1996) Tumor malignancy defined by aberrant glycosylation and sphingo(glyco)lipid metabolism. *Cancer Res. 56*, 5309–5318.

(11) Kotani, M., Kawashima, I., Ozawa, H., Terashima, T., and Tai, T. (1993) Differential distribution of major gangliosides in rat central nervous system detected by specific monoclonal antibodies. *Glycobiology 3*, 137–146.

(12) Kotani, M., Kawashima, I., Ozawa, H., Ogura, K., Ishizuka, I., Terashima, T., and Tai, T. (1994) Immunohistochemical localization of minor gangliosides in the rat central nervous system. *Glycobiology 4*, 855–865.

(13) Sugiura, Y., Shimma, S., Konishi, Y., Yamada, M. K., and Setou, M. (2008) Imaging mass spectrometry technology and application on ganglioside study; visualization of age-dependent accumulation of C20-ganglioside molecular species in the mouse hippocampus. *PLoS ONE 3*, No. e3232.

(14) Chan, K., Lantier, P., Liu, X., Sandhu, J. K., Stanimirovic, D., and Li, J. (2009) MALDI mass spectrometry imaging of gangliosides in mouse brain using ionic liquid matrix. *Anal. Chim. Acta 639*, 57–61.

(15) Colsch, B., and Woods, A. S. (2010) Localization and imaging of sialylated glycosphingolipids in brain tissue sections by MALDI mass spectrometry. *Glycobiology 20*, 661–667.

(16) Goto-Inoue, N., Hayasaka, T., Zaima, N., Kashiwagi, Y., Yamamoto, M., Nakamoto, M., and Setou, M. (2010) The detection of glycosphingolipids in brain tissue sections by imaging mass spectrometry using gold nanoparticles. *J. Am. Soc. Mass Spectrom.*10.1016/j.jasms.2010.08.002.

(17) Costello, C. E., Juhasz, P., and Perreault, H. (1994) New mass spectral approaches to ganglioside structure determinations. *Prog. Brain Res. 101*, 45–61.

(18) Harvey, D. J. (1999) Matrix-assisted laser desorption/ionization mass spectrometry of carbohydrates. *Mass Spectrom. Rev. 18*, 349–450.

(19) O'Connor, P. B., Mirgorodskaya, E., and Costello, C. E. (2002) High pressure matrix-assisted laser desorption/ionization Fournier transform mass spectrometry for minimization of ganglioside fragmentation. *J. Am. Soc. Mass Spectrom. 13*, 402–407.

(20) Jackson, S. N., Wang, H. Y., Woods, A. S., Ugarov, M., Egan, T., and Schultz, J. A. (2005) Direct tissue analysis of phospholipids in rat brain using MALDI-TOFMS and MALDI-ion mobility-TOFMS. *J. Am. Soc. Mass Spectrom. 16*, 133–138.

(21) Woods, A. S., and Jackson, S. N. (2006) Brain tissue lipidomics: Direct probing using matrix-assisted laser desorption/ionization mass spectrometry. *AAPS J. 8*, E391–E395.

(22) Heffer-Lauc, M., Lauc, G., Nimrichter, L., Fromholt, S. E., and Schnaar, R. L. (2005) Membrane redistribution of gangliosides and glycosylphosphatidylinositol-anchored proteins in brain tissue sections under conditions of lipid raft isolation. *Biochim. Biophys. Acta 1686*, 200–208.

(23) Zarei, M., Bindila, L., Souady, J., Dreisewerd, K., Berkenkamp, S., Müthing, J., and Peter-Katalinić, J. (2008) A sialylation study of mouse brain gangliosides by MALDI a-TOF and o-TOF mass spectrometry. *J. Mass Spectrum 43*, 716–725.

(24) Domon, B., and Costello, C. E. (1988) Structure elucidation of glycosphingolipids and gangliosides using high-performance tandem mass spectrometry. *Biochemistry 27*, 1534–1543.

(25) Dzieciatkowska, M., Brochu, D., Van Belkum, A., Heikema, A. P., Yuki, N., Houliston, R. S., Richards, J. C., Gilbert, M., and Li, J. (2007) Mass spectrometric analysis of intact lipooligosaccharide: direct evidence for O-acetylated sialic acids and discovery of O-linked glycine expressed by *Campylobacter jejuni*. *Biochemistry 46*, 14704–14714.

(26) Paxinos, G., Watson, C. (2007) *The Rat Brain in Stereotaxic Coordinates*, 6th ed., Academic Press, San Diego, CA.

(27) Ghidoni, R., Sonnino, S., Tettamenti, G., Baumann, N., Reuter, G., and Schauer, R. (1980) Isolation and characterization of a trisialoganglioside from mouse brain, containing 9-O-acetyl-N-acetylneuraminic acid. *J. Biol. Chem. 255*, 6990–6995.

(28) Chigorno, V., Sonnino, S., Ghidoni, R., and Tettamenti, G. (1982) Isolation and characterization of a tetrasialoganglioside from mouse brain, containing 9-O-acetyl-N-acetylneuraminic acid. *Neurochem. Int. 4*, 531–539.

(29) Sonnino, S., Ghidoni, R., Chigorno, V., Masserini, M., and Tettamentti, G. (1983) Recognition by two-dimensional thin-layer chromatography and densitometric quantification of alkali-labile gangliosides from the brain of different animals. *Anal. Biochem. 128*, 104–114.

(30) Varki, A. (1992) Diversity in the sialic acids. *Glycobiology 2*, 25–40.

(31) Schauer, R. (2009) Sialic acids as regulators of molecular and cellular interactions. *Curr. Opin. Struct Biol. 19*, 507–514.

(32) Ivleva, V. B., Elkin, Y. N., Budnik, B. A., Moyer, S. C., O'Connor, P. B., and Costello, C. E. (2004) Coupling thin-layer chromatography with vibrational cooling matrix-assisted laser desorption/ionization Fourier transform mass spectrometry for the analysis of ganglioside mixtures. *Anal. Chem. 76*, 6484–6491.

(33) Khola, G., Stockfleth, E., and Schauer, R. (2002) Gangliosides with O-acetylated sialic acids in tumors of neuroectodermal origin. *Neurochem. Res. 27*, 583–592.

(34) Folch, J., Lees, M., and Sloane Stanley, G. H. (1957) A simple method for the isolation and purification of total lipids from animal tissues. *J. Biol. Chem. 226*, 497–509.

(35) Williams, M. A., and McCluer, R. H. (1980) The use of Sep-Pak C18 cartridges during the isolation of gangliosides. *J. Neurochem. 35*, 266–269.

(36) Jackson, S. N., Wang, H. Y., and Woods, A. S. (2007) in situ structural characterization of glycerophospholipids and sulfatides in brain tissue using MALDI-MS/MS. *J. Am. Soc. Mass Spectrom. 18*, 17–26.

(37) Franck, J., Arafah, K., Barnes, A., Wisztorski, M., Salzet, M., and Fournier, I. (2009) Improving tissue preparation for matrix-assisted laser desorption ionization mass spectrometry imaging. Part 1: Using microspotting. *Anal. Chem. 81*, 8193–8202.

(38) Sugiura, Y., Konishi, Y., Zaima, N., Kajihara, S., Nakanishi, H., Taguchi, R., and Setou, M. (2009) Visualization of the cell-selective distribution of PUFA-containing phosphatidylcholines in mouse brain by imaging mass spectrometry. *J. Lipid Res. 50*, 1776–1788.